AFRL-RX-TY-TP-2009-4613

SURFACE CHARACTERIZATION AND DIRECT BIOELECTROCATALYSIS OF MULTICOPPER OXIDASES (POSTPRINT)

Dmitri M. Ivnitski, Constantine Khripin and Plamen Atanassov
Chemical and Nuclear Engineering
University of New Mexico
Albuquerque, NM 87131

Heather R. Luckarift
Universal Technology Corporation
1270 North Fairfield Road
Dayton, OH 45432

Glenn R. Johnson
Airbase Technologies Division
Air Force Research Laboratory
139 Barnes Drive, Suite 2
Tyndall Air Force Base, FL 32403-5323

Contract No. FA8650-07-D-5800-0037

(Month) (Year)

AIR FORCE RESEARCH LABORATORY
MATERIALS AND MANUFACTURING DIRECTORATE

■ **Air Force Materiel Command** ■ **United States Air Force** ■ **Tyndall Air Force Base, FL 32403-5323**

REPORT DOCUMENTATION PAGE

Form Approved
OMB No. 0704-0188

PLEASE DO NOT RETURN YOUR FORM TO THE ABOVE ADDRESS.

1. REPORT DATE *(DD-MM-YYYY)*	2. REPORT TYPE	3. DATES COVERED *(From - To)*
31-JAN-2010	Journal Article - POSTPRINT	01-OCT-2008 -- 31-OCT-2009

4. TITLE AND SUBTITLE

Surface Characterization and Direct Bioelectrocatalysis of Multicopper Oxidases (POSTPRINT)

5a. CONTRACT NUMBER

FA8650-07-D-5800-0037

5b. GRANT NUMBER

5c. PROGRAM ELEMENT NUMBER

0602102F

6. AUTHOR(S)

*Ivnitski, Dmitri M.; *Khripin, Constantine; **Luckarift, Heather R.; ^Johnson, Glenn R.; *Atanassov, Plamen

5d. PROJECT NUMBER

4915

5e. TASK NUMBER

L0

5f. WORK UNIT NUMBER

Q140LA62

7. PERFORMING ORGANIZATION NAME(S) AND ADDRESS(ES)

*Chemical and Nuclear Engineering, University of New Mexico, Albuquerque, NM 87131
**Universal Technology Corporation, 1270 North Fairfield Road, Dayton, OH 45432

8. PERFORMING ORGANIZATION REPORT NUMBER

9. SPONSORING/MONITORING AGENCY NAME(S) AND ADDRESS(ES)

^Air Force Research Laboratory
Materials and Manufacturing Directorate
Airbase Technologies Division
139 Barnes Drive, Suite 2
Tyndall Air Force Base, FL 32403-5323

10. SPONSOR/MONITOR'S ACRONYM(S)

AFRL/RXQL

11. SPONSOR/MONITOR'S REPORT NUMBER(S)

AFRL-RX-TY-TP-2009-4613

12. DISTRIBUTION/AVAILABILITY STATEMENT

Distribution Statement A: Approved for public release; distribution unlimited.
Available only to DTIC users. U.S. Government or Federal Purpose Rights License.

13. SUPPLEMENTARY NOTES

Distribution Code 20: JOURNAL ARTICLES; DTIC USERS ONLY. Document contains color images. Published in Electrochimica Acta 55 (2010) 7385–7393.

14. ABSTRACT

Multicopper oxidases (MCO) have been extensively studied as oxygen reduction catalysts for cathodic reactions in biofuel cells. Theoretically, direct electron transfer between an enzyme and electrode offers optimal energy conversion efficiency providing that the enzyme/electrode interface can be engineered to establish efficient electrical communication. In this study, the direct bioelectrocatalysis of three MCO (Laccase from Trametes versicolor, bilirubin oxidase (BOD) from the fungi Myrothecium verrucaria and ascorbate oxidase (AOx) from Cucurbita sp.)wasinvestigated and compared as oxygen reduction catalysts. Protein film voltammetry and electrochemical characterization of the MCO electrodes showed that DET had been successfully established in all cases. Atomic force microscopy imaging and force measurements indicated that enzyme was immobilized as a monolayer on the electrode surface. Evidence for three clearly separated anodic and cathodic redox events related to the Type 1 (T1) and the trinculear copper centers (T2, T3) of variousMCOwasobserved. The redox potential of the T1 centerwasstrongly modulated by physiological factors including pH, anaerobic and aerobic conditions and the presence of inhibitors.

15. SUBJECT TERMS

laccase, bilirubin oxidase, ascorbate oxidase, bio-cathode, exnymatic fuel cell

16. SECURITY CLASSIFICATION OF:			17. LIMITATION OF ABSTRACT	18. NUMBER OF PAGES	19a. NAME OF RESPONSIBLE PERSON
a. REPORT	b. ABSTRACT	c. THIS PAGE			Glenn R. Johnson
U	U	U	UU	9	19b. TELEPHONE NUMBER *(Include area code)*

Reset

Standard Form 298 (Rev. 8/98)
Prescribed by ANSI Std. Z39.18

Electrochimica Acta 55 (2010) 7385–7393

Contents lists available at ScienceDirect

Electrochimica Acta

journal homepage: www.elsevier.com/locate/electacta

Surface characterization and direct bioelectrocatalysis of multicopper oxidases

Dmitri M. Ivnitski[a,b,*], Constantine Khripin[a], Heather R. Luckarift[b,c], Glenn R. Johnson[b], Plamen Atanassov[a,**]

[a] Chemical and Nuclear Engineering, University of New Mexico, Albuquerque 87131, USA
[b] Air Force Research Laboratory, AFRL/RXQL, Microbiology and Applied Biochemistry, Tyndall Air Force Base, FL 32403, USA
[c] Universal Technology Corporation, 1270 N. Fairfield Road, Dayton, OH 45432, USA

ARTICLE INFO

Article history:
Received 13 April 2010
Received in revised form 9 July 2010
Accepted 10 July 2010
Available online 17 July 2010

Keywords:
Laccase
Bilirubin oxidase
Ascorbate oxidase
Bio-cathode
Enzymatic fuel cell

ABSTRACT

Multicopper oxidases (MCO) have been extensively studied as oxygen reduction catalysts for cathodic reactions in biofuel cells. Theoretically, direct electron transfer between an enzyme and electrode offers optimal energy conversion efficiency providing that the enzyme/electrode interface can be engineered to establish efficient electrical communication. In this study, the direct bioelectrocatalysis of three MCO (Laccase from *Trametes versicolor*, bilirubin oxidase (BOD) from the fungi *Myrothecium verrucaria* and ascorbate oxidase (AOx) from *Cucurbita* sp.) was investigated and compared as oxygen reduction catalysts. Protein film voltammetry and electrochemical characterization of the MCO electrodes showed that DET had been successfully established in all cases. Atomic force microscopy imaging and force measurements indicated that enzyme was immobilized as a monolayer on the electrode surface. Evidence for three clearly separated anodic and cathodic redox events related to the Type 1 (T1) and the trinuclear copper centers (T2, T3) of various MCO was observed. The redox potential of the T1 center was strongly modulated by physiological factors including pH, anaerobic and aerobic conditions and the presence of inhibitors.

1. Introduction

Progress in nanoscience and nanotechnology has created an excellent basis for design and development of the next generation of biofuel cells based on direct electrical communication between the active site of enzymes and an electrode [1–11]. Direct electron transfer (DET) between enzyme catalysts and electrode materials contributes significant design advantages in the construction of biofuel cells. A biofuel cell based on DET can theoretically operate in a single compartment cell, without exogenous electron transfer redox mediators, and at a potential approaching the redox potential of the enzyme itself. In addition, DET provides the opportunity to simplify and miniaturize the construction of biofuel cells for integration into microscale sensor transmitter systems, pacemakers, and lab-on-a-chip devices [12–14].

Multicopper oxidases (MCO) have been extensively studied in an attempt to harness the biochemical reduction of molecular oxygen to generate electrical energy. Direct electrical communication between laccase and an electrode was first demonstrated over 30 years ago [15]. Since that time, a series of publications related to direct electrical communication between redox enzyme molecules and electrodes in the absence and in the presence of different promoters have been reported [16–21]. The electroreduction of dioxygen catalyzed by MCO, in the absence of mediators, has now been demonstrated on various electrode surfaces, but the power conversion efficiency remains inherently low [14,22–32]. Optimal conditions for efficient direct bioelectrocatalysis depend upon a combination of factors including: the electrode material, enzyme orientation and proximity to the electrode surface, and the location of the enzyme redox centers in relation to enzyme structure [8,9,17,18,33,34]. Ideally, the electron tunneling distance of the redox centers should be minimized such that the enzymes biocatalytic reaction is the only limiting process [33,35]. One of the challenges, however, is that the redox centers of enzyme molecules are located deep inside the protein structure; leading to a long electron tunneling distance between the enzyme and the electrode and thus inefficient electron transfer. Secondly, there are difficulties associated with engineering the enzyme/electrode interface to establish electron transfer (ET) between enzyme and electrode. As such, a detailed understanding of the enzyme electrode interface, the intermolecular and intramolecular ET mechanisms, along with methodological principals to reduce the electron tunneling distance between enzyme and electrodes still need to be understood, before DET can be optimized to enhance biofuel cell productivity.

In this study, the direct bioelectrocatalysis of MCO is investigated as an integral step in understanding the design and

* Corresponding author at: Chemical and Nuclear Engineering, University of New Mexico, Albuquerque 87131, USA. Tel.: +1 505 277 7952; fax: +1 505 277 4935.
** Corresponding author. Tel.: +1 505 277 2640; fax: +1 505 277 5433.
E-mail addresses: ivnitski@unm.edu (D.M. Ivnitski), plamen@unm.edu (P. Atanassov).

0013-4686/$ – see front matter © 2010 Elsevier Ltd. All rights reserved.
doi:10.1016/j.electacta.2010.07.026

development of bio-cathodes for biofuel cells. Laccase from *Trametes versicolor*, bilirubin oxidase (BOD) from the fungi *Myrothecium verrucaria* and ascorbate oxidase (AOx) from *Cucurbita* sp. were selected as representative MCO. Despite the differing substrate specificity of these three enzymes, each MCO includes Type 1 (T1), Type 2 (T2), and Type 3 (T3) redox copper centers [34,36–38]. The T1 redox center provides long range interfacial ET from the electrode and intramolecular ET to the trinuclear redox copper center, which in turn plays a key role in the reduction of oxygen to water [38–40]. It is well documented that the copper ions in the redox center of MCO catalyze ET reactions by switching their oxidation states between Cu(II) and Cu(I). Therefore, an important thermodynamic parameter of the MCO is the redox potential of the copper centers of the enzymes. The majority of electrochemical studies of MCO, however, show variable values for redox responses [25,41,42]. The redox potential of the T1 copper center, for example, can range from 0.23 V to 0.59 V (vs. Ag/AgCl) for laccases from different species [43]. Potentiometric titration and spectrophotometry of a plant laccase from *Rhus vernicifera*, for example, revealed three distinct electron-accepting sites in the molecule. The T1 copper is associated with a strong absorption band at 614 nm and has a potential of 0.22 V (vs. Ag/AgCl). T2 copper has a lower potential, 0.19 V, and T3 has a reported potential of 0.26 V (vs. Ag/AgCl) at pH 7 [44]. The redox potentials of the T2 and T3 sites of fungal laccase from *Trametes* sp., however, differ significantly from the *R. vernicifera* plant laccase, which makes direct comparisons difficult [43]. Similarly, ET processes in the low and high potential range, 0.2 V and 0.47 V (vs. Ag/AgCl), respectively, were seen for BOD from *M. verrucaria* [45]. The formal redox potential of T1 of BOD was found to be 0.26 V (vs. Ag/AgCl) at pH 5.3, but other studies reported potentials more positive than 0.48 V (vs. Ag/AgCl) at pH 7 [45–47]. Evidence of DET for AOx has also been recently reported in the literature, but only a single redox response was detected in the cathodic and anodic waves of AOx, although several redox centers are known to be present in the enzyme [48–50].

Thus, it is still a challenge to determine true redox potential values for T1, T2, and T3 redox centers of differing MCO. The difficulties in determining accurate redox potentials are associated primarily with irreproducible assembly of biomolecules into functional architectures on the electrode surface. Many factors, however, including electrode material and treatment, method of enzyme immobilization, distance between redox centers of enzymes and electrode, specific enzyme orientation, ionic strength and pH of the buffer solution, all contribute to the relative potential values of the anodic and cathodic peaks of the redox centers of the enzyme. Recent studies have indicated that the protein dynamics of MCO are also an important factor in controlling the interfacial and intramolecular ET [51]. Variations in redox potentials may be attributed to non-covalent binding of copper ions in the active site of the MCO, whereby changes in hydrogen bonding around the copper ions may affect the bond lengths between the copper atoms and coordinating histidine residues [52]. It is necessary, therefore, to know specific redox properties, conformation perturbations, fluctuations and rearrangement of enzyme molecules directly on the electrode surface. Characterization of MCO using a protocol that provides direct comparison of the enzyme and electrode interface would therefore provide a useful tool in bioelectrode development.

Herein, to extract new information about the redox properties of the active site interaction of MCO (laccase, BOD and AOx) a protein film voltammetry (PFV) approach has been applied which essentially relies on the assembly of enzyme molecules as a monolayer directly onto an electrode surface [53–55]. Because the MCO form a monolayer on the electrode surface, the active sites are theoretically accessible to species in solution (oxygen, protons, redox mediators and catalytic substrates) allowing for direct observation of coupled reactions. In addition, the physical architecture of enzyme films on the electrode surface was investigated by atomic force microscopy (AFM). AFM provides high surface sensitivity and non-destructive characterization of protein interactions and structural information, to single enzyme molecule resolution, and can be used to directly quantify protein on the electrode surface [28,56–58].

2. Experimental

2.1. Materials

Laccase from *T. versicolor*, bilirubin oxidase (BOD) from the fungus *M. verrucaria*, ascorbate oxidase (AOx) from *Cucurbita* sp., bathocuproine disulfonate (BCS), glutaraldehyde (GA) and dimethyl sulfoxide (DMSO) were purchased from Sigma (St. Louis, MO). Dithiobis (succinimidyl propionate) (DSP) was purchased from Pierce (Thermo Scientific, Rockford, IL). All other chemicals were of analytical grade and obtained from various commercial sources. All solutions were prepared with deionized water. Screen-printed carbon (SP-C) electrodes were obtained from PINE Instruments (Raleigh, NC).

2.2. Immobilization of MCO on screen-printed electrodes

Laccase from *T. versicolor* was purified by dialysis at 4 °C (3 exchanges of 1 L HEPES buffer; 10 mM, pH6) containing Cu_2SO_4 (10 mM). Dialyzed protein was stored in aliquots at −20 °C. Protein concentration was determined by bicinochinic acid protein assay using directions provided by the manufacturer (Pierce Biotechnology, Rockford, IL). Stock solutions of BOD and AOx were prepared to known concentrations and used without further purification.

Two approaches for enzyme immobilization on SP-C were investigated: (1) covalent attachment by GA and (2) creation of a self-assembled monolayer using DSP. For GA immobilization, the surface of a SP-C electrode was treated with 25% GA for 1 h and then washed extensively with phosphate buffer (0.1 M, pH 7.0) and dried under nitrogen. Adsorbed GA molecules were used to create a stable monolayer of enzyme molecules by lateral cross-linking. MCO (30 μL of 1 mg mL^{-1} in 0.1 M phosphate buffer, pH 7.0) was applied to the surface of the GA-modified SP-C electrode and incubated for 2 h at room temperature.

To prepare DSP-functionalized electrodes, cleaned SP-C electrodes were activated by adding DSP (10 μL of a 4 mg mL^{-1} solution, prepared in DMSO) to the carbon surface for 1 h at room temperature. The electrode was washed with DMSO to remove unbound DSP and dried under nitrogen. MCO (30 μL of a 1 mg mL^{-1} solution in 0.1 M phosphate buffer, pH 6.8) was then added to the electrode and incubated for 2 h at room temperature. The MCO functionalized electrodes were washed with phosphate buffer (0.1 M, pH 5.8) and stored in the same buffer at 4 °C.

2.3. Atomic force microscopy

AFM imaging was carried out on an MPF3D – Bio AFM from Asylum Research (Santa Barbara, CA). Imaging was performed in tapping mode using SiN cantilevers (Olympus TR400PSA, Asylum Research) with filtered phosphate buffer (0.1 M, pH 6.8). A drop of buffer was placed on the electrode and the cantilever was immersed in the buffer directly. Typical imaging settings were 300 mV free amplitude and 100 mV set-point in tapping mode at 2 Hz scan rate. Force curves were collected after acquiring an image in tapping mode.

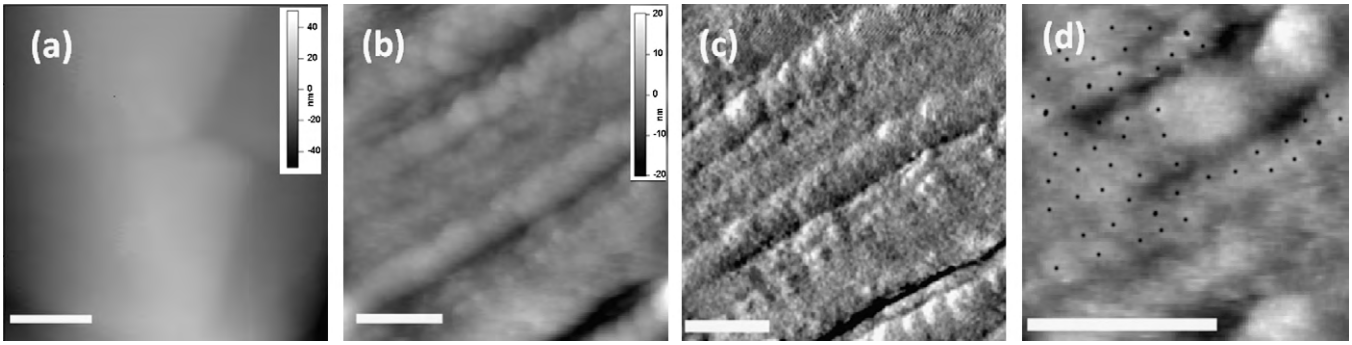

Fig. 1. Tapping mode AFM images of laccase on a SP-C electrode, in liquid: height (b), amplitude (c) and expanded section (d) showing enzyme molecules marked by black dots. Scale bars are 50 nm. An uncoated electrode is included for comparison (a).

2.4. Protein film voltammetry

PFV analysis was performed using a potentiostat/galvanostat (EG&G/Princeton Applied Research, Oak Ridge, TN, model 263A) connected to a personal computer. In all experiments a one-compartment electrochemical cell (5 mL volume) consisting of the enzyme-modified SP-C electrode, SP counter electrode and standard Ag/AgCl reference electrodes were used. The surface area of the working electrode was 0.13 cm^2. At the start of the experiments, nitrogen or oxygen was bubbled through the buffer solution for 40 min. The cyclic voltammograms (CVs) of enzyme electrodes were measured in the absence (anaerobic) and presence (aerobic) of oxygen with a potential scan from −0.2 V to +0.9 V vs. Ag/AgCl. All electrochemical experiments were carried out at 20 ± 0.5 °C.

3. Results and discussion

3.1. Surface analysis of absorbed laccase by tapping mode AFM

Analysis of the bioelectrode surface by AFM confirmed that the MCO were adsorbed to the carbon electrode surfaces as a monolayer (Fig. 1). Phase-contrast imaging clearly resolved the deposited protein from the electrode surface. Amplitude images provided contrast between materials whilst height analysis provides topographic information (Fig. 1) [59,60]. AFM characterization of the bioelectrodes in liquid highlighted the in situ enzyme/electrode morphology. The use of AFM as a tool for visible characterization of the bio-nano interface, as described, provides critical understanding of the influence of morphology on the bioelectronic processes, and is a versatile approach with further application in bioelectrochemistry [61]. AFM imaging of the SP-C electrodes in aqueous conditions with GA-bound laccase (Fig. 1) revealed a series of tightly packed protein particles, indicative of homogenous enzyme loading on the electrode surface. The average particle spacing was 8 ± 1 nm, consistent with the reported size for laccase [37,38]. The area per enzyme was calculated to be 66 ± 14 nm^2. The theoretical area of the enzyme is 33 nm^2 per molecule, indicating a percent surface coverage on the electrode of ∼50%. This correlates well with the 52.5% predicted for squares by random sequential adsorption theory and suggests that adsorption of enzyme molecules on the SP-C electrode surface is an irreversible sequential process that produces a well-defined monolayer [62]. Visual marking of the enzyme molecules qualitatively reveals ordered protein adsorption (Fig. 1d). Similar surface coverage was observed for laccase bound to SP-C via DSP (measured particle area of 65 ± 7 nm^2 and a percent surface coverage of ∼49%; data not shown) indicating that the enzyme loading efficiency was not significantly affected by the immobilization chemistry.

The AFM force curve measurements corroborate the protein density and protein film thickness found in liquid AFM images. The force curve for the bare SP-C electrode is similar to an ideal rigid surface, as expected (Fig. 2a). The force curve for an SP-C electrode with GA-bound laccase differs at the area of initial contact indicating that the tip encountered initial resistance, which it overcame with a force on the order of 0.5 nN and after compression of several nanometers encountered a rigid surface, confirming a soft layer of several nanometers of protein absorbed on the hard carbon electrode.

An isolated object of diameter d and height n has apparent diameter D given by:

$$D = d + 2\sqrt{r^2 - (r-n)^2} \quad (1)$$

where r is the radius of the tip, assuming the protein to be rigid and much smaller than the tip radius (the manufacturer's specification for the tip radius is 15 nm, giving an apparent diameter of 26 nm for an enzyme of approximately 4.5 nm). In practice, enzymes are seldom perfectly isolated and not rigid; therefore this can be viewed as an upper limit for observed diameter. On the other hand, for close-packed objects the correct size will be observed. The histogram of observed particle size on SP-C electrode confirms an homogenous coating with an average diameter of ∼8 nm (Fig. 2b), irrespective of the immobilization chemistry used (GA or DSP) and again, is in good agreement with the reported diameter for laccase of 7 nm [37]. The current per enzyme molecule was calculated to be 5×10^{-11} μA [using measured values of observed electric current, electrode surface area of 0.13 cm^2 based on capacitance measurements and enzyme density (calculated from the average area per enzyme molecule derived by AFM)].

3.2. Direct electrochemistry of MCO on SP-C electrode

Theoretically, a key requirement for direct bioelectrocatalysis is to minimize the distance between the redox centers of MCO and the electrode. Direct enzyme immobilization onto a GA-modified surface allows for the ordered formation of a homogenous enzyme monolayer (as observed by AFM) that corresponds to the requirements of the PFV method [53–55]. Despite the ordered macromolecular immobilization of protein, the specific orientation of MCO molecules on the electrode surface is still inherently random. As such, MCO molecules may be positioned in any combination of conformational orientations, for example, placing the T1 copper center closest to the electrode surface, or alternatively, positioning the trinuclear copper center in close alignment with the electrode. Thus, the electrochemistry observed by PFV is a snapshot of the 'average' and cumulative redox events of all three redox centers (T1, T2 and T3), rather than specifically related to one single molecular orientation.

The results from CV measurements provide detail about the interfacial electronic connections between the MCO and the elec-

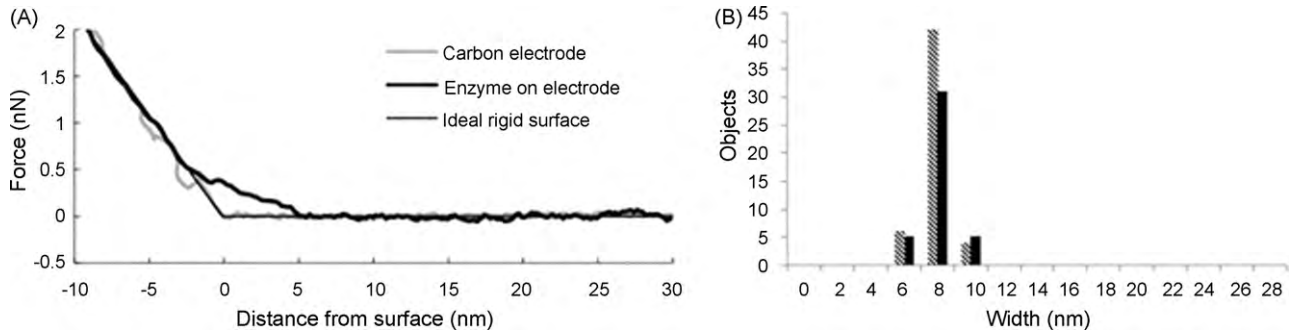

Fig. 2. (A) Force curves on unmodified and laccase-modified SP-C electrode. Note: a force curve for an ideal rigid surface, consisting of two perfectly straight lines, is included for reference; (B) histogram of observed enzyme particle size on SP-C electrode; with DSP (solid columns) and GA (hashed columns) functionalization.

trode surface (Figs. 3 and 4). Evidence for distinct and often reversible redox events for each MCO electrode suggests that the proteins were randomly orientated on the electrode in such a way that the T1, T2, and T3 copper atoms could accept or pass electrons to the electrode at appropriate potentials. CV traces in the presence

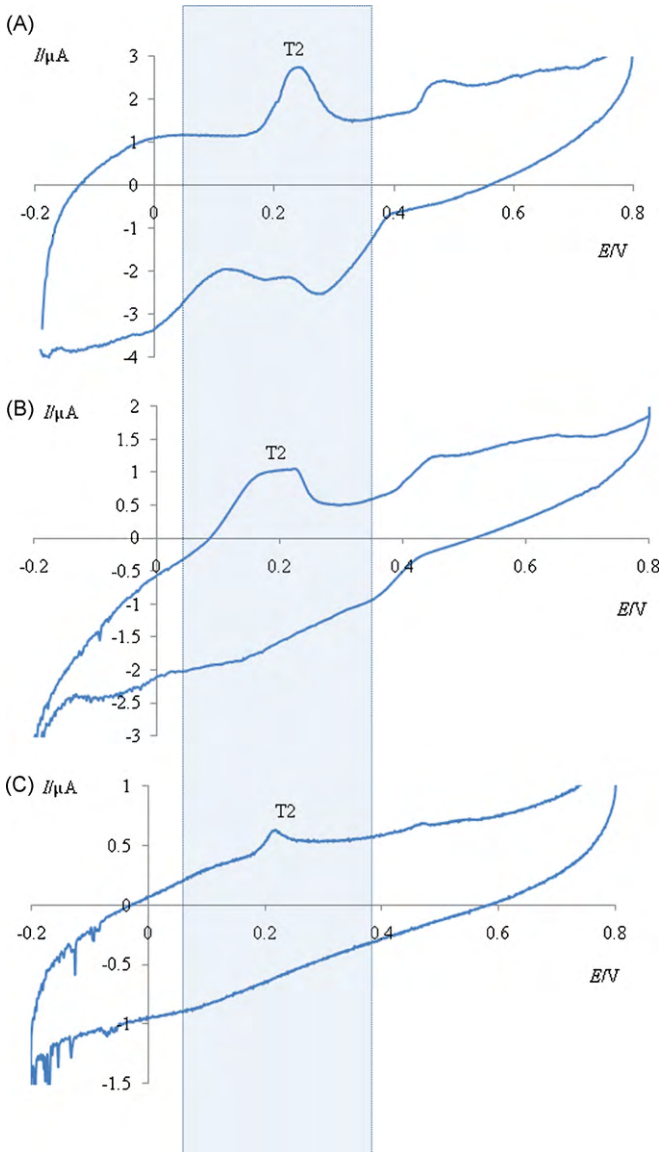

Fig. 3. CVs of MCOs on SP-C electrodes. (A) Laccase, (B) BOD and (C) AOx. CV measurements in phosphate buffer (0.1 M, pH 6.8 for AOx, pH 5.8 for BOD and laccase) at a scan rate of 10 mV/s under anaerobic conditions.

of nitrogen, show strong redox events at ~0.2 V in all cases and were attributed to the T2 copper center, in agreement with previous studies (Fig. 3). The redox potential of the T2 copper center is strictly conserved across the three MCO tested. The lack of variation in redox potential likely results from the high level of similarity between the amino acid sequences (and hence protein structure) at the regions surrounding the T2 redox center from the different MCO [63]. Redox events that occur in the absence of oxygen are attributable to direct communication between the enzyme and the electrode surface.

CV measurements in aerobic conditions demonstrate redox events due to inter- and intra-molecular electron transport that follow as a direct result of oxygen reduction. Faradic currents increase as expected in the presence of oxygen as a result of the transfer of four electrons from the electrode to the T1 copper center. High current density under aerobic conditions is in agreement with previous reports for laccase and BOD, and further supports using MCO as catalysts in enzyme-based fuel cells [10,31,64–66]. CV scans show well-separated Faradic processes for all three MCO enzymes (Fig. 4). The anodic and cathodic peaks that correspond to the enzyme redox centers were apparent in three distinct potential areas; low (0.0–0.3 V), mid (0.3–0.5 V) and high (0.5–0.8 V) (vs. Ag/AgCl) (Fig. 4). The present data and previous studies by our research group and others all indicate that the redox event at a high potential area between 0.5 V and 0.8 V corresponds directly to the T1 redox copper center [63,64]. In all cases, the anodic peak corresponding to the T1 site is observed but the corresponding cathodic peak is not. This is attributed to the rapid oxidation of copper ions in the redox centers that is countered by a much slower corresponding reduction event, due to the slow kinetics of intramolecular electron transfer [63]. The formal redox potentials for T1 copper centers were determined from midpoint oxidation/reduction potentials as 0.55 ± 0.02 V vs. Ag/AgCl for BOD and 0.52 ± 0.04 V vs. Ag/AgCl for laccase (see Fig. 4). These observations were reproducible across replicate electrodes. The present values are in good agreement with redox potential values for the T1 center previously determined for fungal laccases [10,38,47]. Based on our consistent observations, the redox potential of the T1 copper center correlates well with the onset potential of oxygen reduction, and with the open circuit potential (OCP) obtained in aerobic conditions. The laccase electrodes, for example, produced an OCP of 0.56 ± 0.04 V, which corresponds precisely with the onset of oxygen reduction. Similarly, for BOD, an OCP of 0.55 V correlates with the onset potential for oxygen reduction. It is clear from this correlation that (i) the redox potential of the T1 copper center, (ii) the onset potential of oxygen reduction and (iii) the OCP (under aerobic conditions) are all intimately related and as such, can be used as a definitive measurement of the true redox potential of the T1 copper center.

For AOx, the assignment of the T1 copper is less clear; redox events were observed at 0.48 ± 0.04 V and at ~0.6 V. In previous

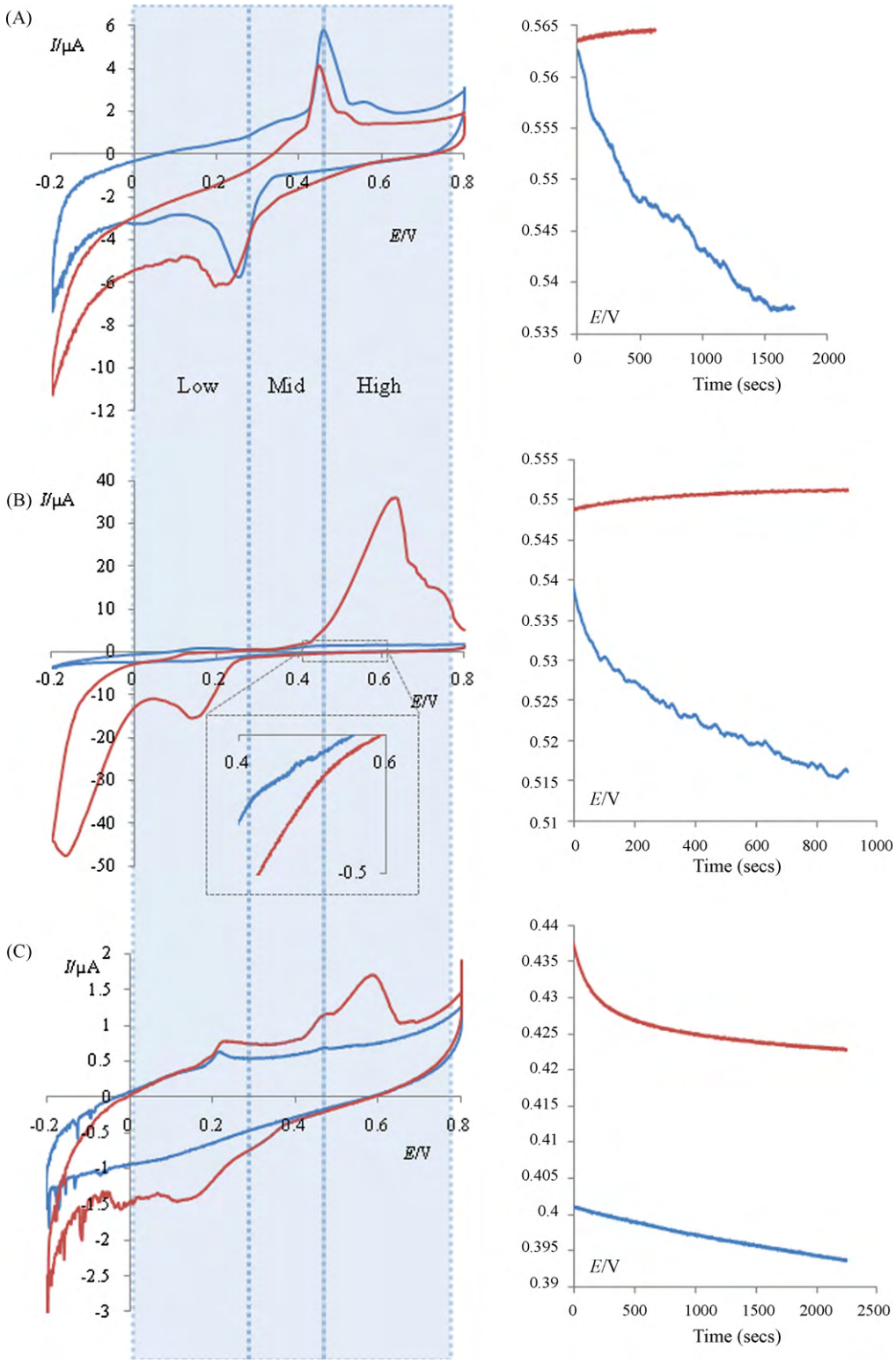

Fig. 4. Left panel: CVs of MCOs on SP-C electrodes. (A) Laccase, (B) BOD and (C) AOx. CV measurements in phosphate buffer (0.1 M, pH 6.8 for AOx, pH 5.8 for BOD and laccase) at a scan rate of 10 mV/s under anaerobic (blue line) and aerobic (red line) conditions. Right panel: open circuit potential of same electrodes under anaerobic (blue line) and aerobic (red line) conditions (vs. Ag/AgCl). Inset in CV (panel B) is enlarged area to show onset of oxygen reduction. (For interpretation of the references to color in this figure legend, the reader is referred to the web version of the article.)

studies, however, only a single redox response was observed at 0.19 V (vs. Ag/AgCl at pH 5.5) that was attributed to the T1 redox center, although a clear distinction between T1 and T2/T3 complex in the system could not be unequivocally assigned [50]. We now suggest that the lower potential area for AOx corresponds to the trinuclear copper of the enzyme and not to T1 (vide infra). The onset of oxygen reduction in AOx begins at ~0.42 V, again in agreement with the OCP. By analogy to the other MCO, we speculate that the T1 copper center is centered at a redox potential of 0.4 V, which is significantly higher than previous assignations for T1 in AOx.

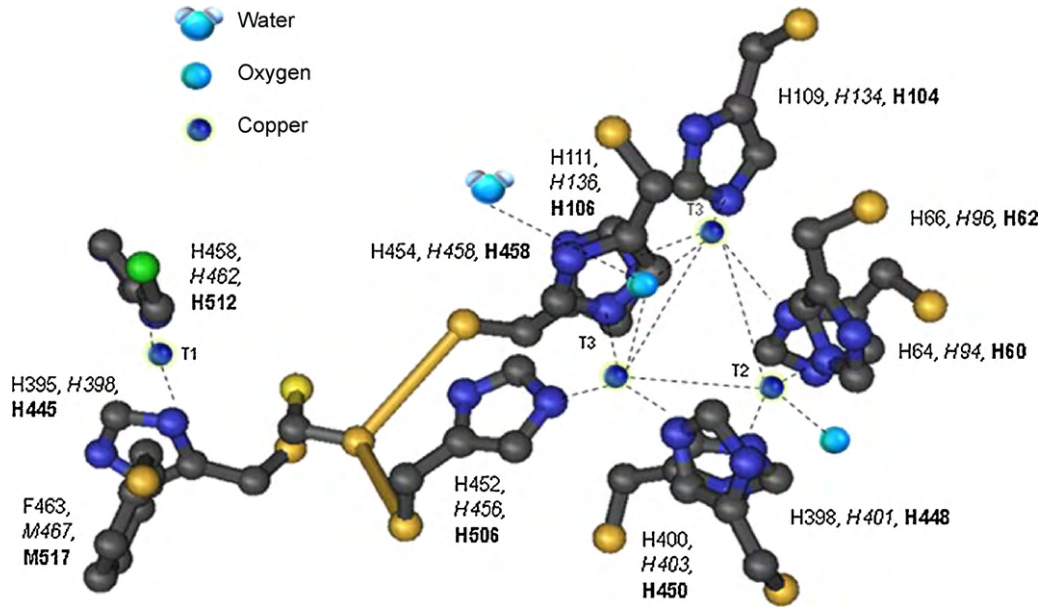

Fig. 5. Schematic illustration of the structure of the MCO active site. Ball and stick representation of the T1 and T2/T3 copper binding sites of laccase from *T. versicolor* (NCBI protein data bank: 1GYC from *T. versicolor*) viewed using Cn3D ver. 4.1 (NCBI). Corresponding amino acid for laccase from *T. versicolor* (plain text), BOD (italics) and AOx from *Cucurbita* sp. (bold) are based on the protein sequence alignment from Sakurai and Kataoka and Shimizu et al. [81,82].

Redox peaks in the potential area below 0.5 V are attributed to DET between the trinuclear redox copper center of MCO and the electrode. Questions remain, however, as to how to discriminate the individual redox potentials of the T2 and T3 copper sites of MCO. Based on the structure of MCO derived from crystallographic data, the structure and co-ordination of the trinuclear copper center is well conserved for MCO (Fig. 5). In all MCO, the T1 redox copper center communicates directly with the T3 redox copper center through orbital overlapping [65,67–69]. Theoretical calculations performed by Kyritsis et al. [70], for AOx indicated that the intramolecular ET from T1 to T3 provides the four electrons for oxygen reduction and that the reduction of the T2 copper center follows directly as a second step in ET [69,71]. According to Marcus theory, the efficiency of ET between two redox centers depends on three main factors; the orbital overlapping matrix, the potential difference between the redox centers, and the distance between the redox sites of the enzyme [33,35]. Inherently, electron tunneling is more efficient through bonded orbitals than through space because the potential barrier is effectively lower. As such, recent studies have demonstrated strong evidence that reduction of the T2 and T3 copper sites requires specific activation for efficient electron transfer to occur. Reduction of the T3 before T2 would result in protonation of the OH^- bridge, and subsequent loss of electronic coupling between T2 and T3 [72].

The prior assignment of T2 at ~0.2 V, leads us to speculate that in all cases, anodic and cathodic redox peaks at the potential area between 0.3 V and 0.5 V belongs to the T3 copper center and that the redox process in the more negative potential area (0.0–0.3 V) belongs to the T2 copper center. This is in agreement with mechanistic studies that show a lower redox for T2 that allows for a transfer of electrons to the T3 copper poised at a higher redox potential. Based on these assumptions, the assigned values of formal redox potentials for T1, T2, and T3 redox copper centers of laccase, BOD and AOx are presented in Table 1.

3.3. Effect of pH on the electrochemistry of MCO on SP-C electrodes

The solution pH during electrochemistry inherently affects the electrochemical behavior of MCO [69,73]. Because native enzyme activity and structure are maintained during PFV, the approach facilitated experiments to define the bio-electrochemical effects based on changes in reaction conditions (pH, oxygen and the influence of enzyme inhibitors). The value of anodic and cathodic peaks for the assigned T1 copper center of AOx, for example, is strongly modulated by pH (Fig. 6). The potential of the T1 anodic peak for AOx was highest (0.66 ± 0.02 V vs. Ag/AgCl) at pH 6.8 (Fig. 6c, trace 3), which corresponds with the pH optimum of the enzyme. At lower pH (4.5 and 5.8), the potential shifts to ~0.48 V (Fig. 6c, trace 1 and 2). At higher pH (8.2), the onset potential for T1 in AOx shifts significantly to a much lower potential of 0.35 V (vs. Ag/AgCl) (Fig. 6c, trace 4). The strong modulation of the redox potential of T1 by pH may be attributed to perturbations in the protein structure in the vicinity of the T1 center and provides further evidence for the assignment of T1 to a potential of ~0.4 V in AOx. Protein dynamics have recently been recognized as a critical parameter in controlling interfacial and intramolecular ET reactions [73,74]. The protein pocket that contains the T1 copper center is a flexible structural component, which allows for variations in redox potential and substrate specificity. Small internal conformational changes in the protein pocket and around the T1 copper center may contribute significantly to the rate-limiting process of ET. In contrast, the redox potential of the trinuclear copper center (T2/T3) is conserved, stable and varies little with changes in environmental conditions (Fig. 6). Previous studies have indicated that the redox potential of the T1 copper does not directly influence the redox state of the trinuclear copper cluster in laccase [69,73]. However, spectroscopic data does show changes in the electronic and geometric structure of T1 coupled to changes in the redox state and co-ordination of the trinuclear copper center [73,74].

Table 1
Measured redox potentials and putative assignment of copper centers in MCO.

Redox copper center	Laccase, $E^{o'}$ (V)	BOD, $E^{o'}$ (V)	AOx, $E^{o'}$ (V)
T1	0.520 ± 0.04	0.546 ± 0.02	0.420 ± 0.04
T2	0.197 ± 0.03	0.217 ± 0.02	0.153 ± 0.03
T3	0.360 ± 0.03	0.385 ± 0.02	n/d

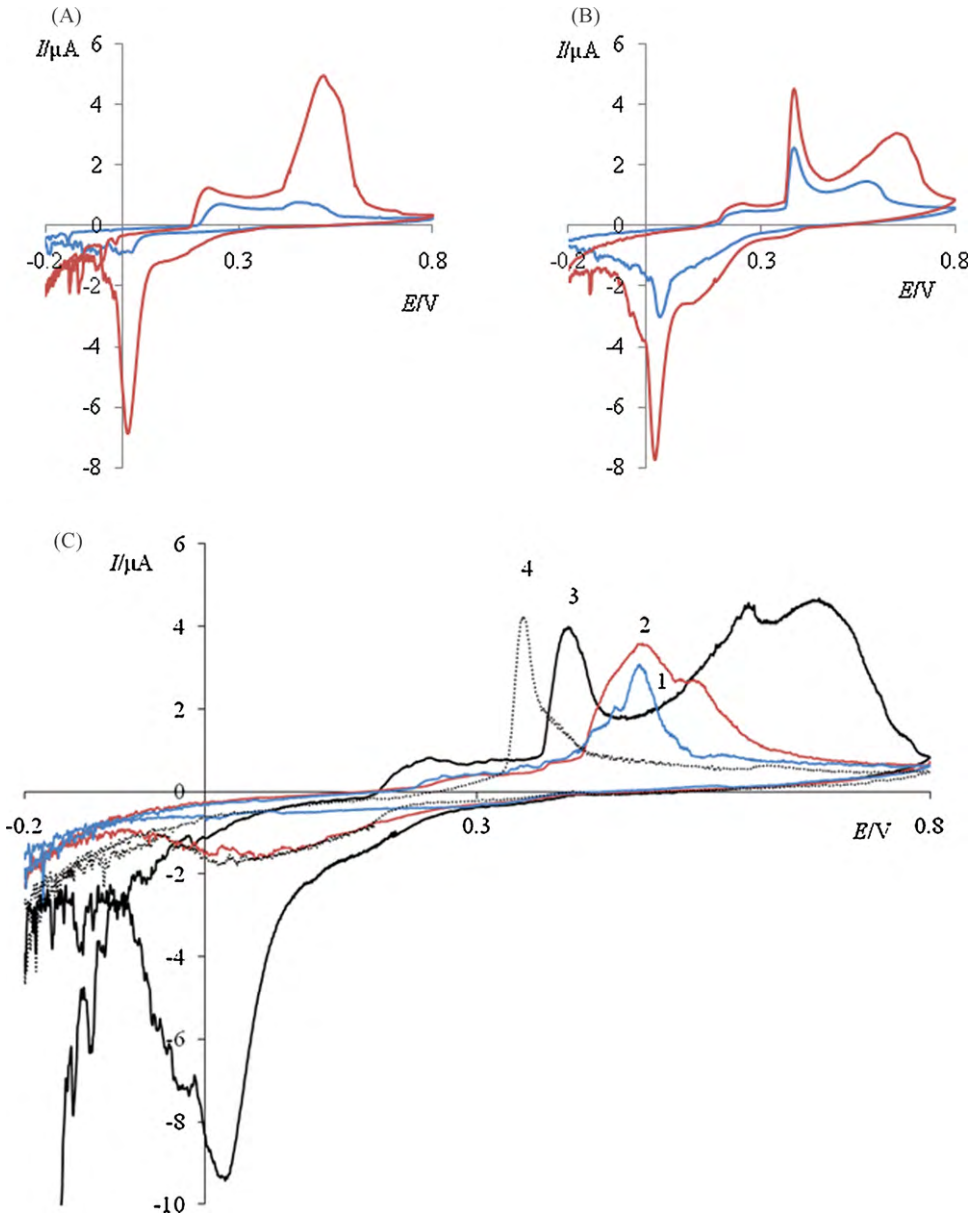

Fig. 6. CVs of AOx on SP-C (GA-functionalized) electrodes. Scan rates of 10 mV/s in phosphate buffer (0.1 M) at a range of pH values. (A) pH 5.8 and (B) pH 7.0 under aerobic (red line) and anaerobic (blue line) conditions. (C) pH 4.5 (1), 5.8 (2), 6.8 (3) and 8.2 (4) under aerobic conditions only. (For interpretation of the references to color in this figure legend, the reader is referred to the web version of the article.)

3.4. *Effect of inhibitors on the electrochemistry of MCO*

The effect of inhibitors on the kinetics of intramolecular ET provided direct evidence on the redox chemistry of the copper centers in MCO. MCO are inhibited by the presence of bathocuproine disulfonate (BCS) which chelates copper (I) ions and creates a strong $(BCS)_2$–Cu(I) complex [75,76]. After a relatively short incubation time with BCS (~30 min) the redox peaks of AOx are diminished significantly (Fig. 7A). Since BCS is a relatively large organic compound, interaction with the enzyme molecule theoretically occurs initially at the substrate binding site of AOx; located near the T1 copper center [36,75–77]. After extended incubation, however, the BCS percolates into the protein interior and eliminates all of the redox character of AOx. A similar effect was reported for analysis of BOD in the presence of BCS [66].

Similarly, changes in the redox state of MCO are observed at low concentrations of chloride and azide ions (Fig. 7B). From the crystal structure of laccase, it is known that oxygen has access to the trinuclear copper center through a solvent channel that permits direct access of dioxygen and water molecules, as well as water-soluble molecules and ions (including inhibitors and redox mediators) [37]. Although, the percolation of BCS into the protein may be limited by the molecule's size, MCO inactivation in the presence of azide and chloride ions is more likely due to the rapid accumulation of the ions inside the solvent-accessible channels of the trinuclear copper center. Messerschmidt et al., for example, showed that two azide ions bind to one of the T3 copper ions. Since the T1 copper is located close to the surface of the enzyme molecule (about 6.5 Å below the surface of the enzyme near the substrate binding site of MCO), the access of inhibitors (azide and chloride ions) to the T1 copper is relatively easy [36]. Accordingly, the significant and rapid changes to the AOx redox event at ~0.4 V, further supports the assignment of this redox potential to the T1 site in AOx. Apparent inhibitor interactions eventually occur at both the T1 and trinuclear copper

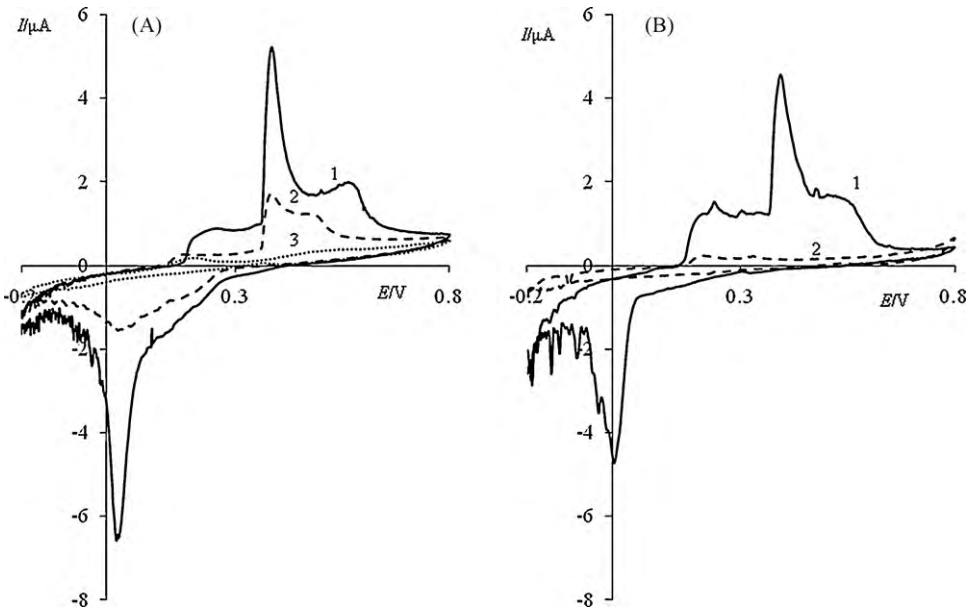

Fig. 7. CV of AOx on SP-C electrodes in the presence of inhibitors. (A) AOx without (1) and with addition of bathocuproine disulfonate (2 mM) for 30 min (2) and overnight (3). Scan rate of 10 mV/s in phosphate buffer (0.1 M, pH 6.8). (B) Without (1) and with (2) addition of 2 mM sodium azide. Scan rate of 10 mV/s in phosphate buffer (0.1 M, pH 6.8).

centers, at which point the intramolecular hopping ET probably switches to a non-hopping mechanism, which effectively blocks oxygen reduction [78–80]. Therefore, the inhibitory effect can be explained in terms of accumulation of inhibitors inside the solvent channel of the T1 and T3 copper centers of MCO, which following the release of bridging oxygen effectively blocks the reduction of oxygen to water. Hence, oxygen reduction was also eliminated for AOx in the presence of inhibitors (Fig. 7).

4. Conclusions

The AFM surface characterization and direct electrochemistry of the three redox copper centers of MCO have been used together to provide insight to ET and protein dynamics. AFM imaging of enzyme-modified electrodes provided direct analysis of enzymes on an electrode surface. The height of individual objects was consistent with the reported size of MCO molecules and indicated that the enzyme adsorbed to the electrode surface in the form of a packed and well-organized monolayer.

PFV revealed clearly separated anodic and cathodic peaks related to the T1 and the trinuclear copper centers of MCO were observed for the first time. The nature of the physiological microenvironment significantly influenced the potential that corresponded to each of the redox centers of MCO. The maximum values of the T1 redox potential and catalytic current for MCO, for example, were measured at pH values that corresponded to the pH optima of the proteins. The redox potential of T1, changed in response to pH, anaerobic and aerobic conditions and the presence of inhibitors. The modulation of the T1 potential is attributed to perturbations of the protein structure and flexible non-covalent binding of copper ions in the MCO active site. As such, stabilization of the T1 redox center is critical for efficient interfacial and intramolecular ET of MCO.

Information garnered from the systematic study of the MCO bioelectrochemistry provides essential guidance for the development of biofuel cell cathodes based on DET of MCO. The properties of MCO redox centers and information on electrode surface interactions may be used for effective engineering of microscale, non-mediated, biofuel cells.

Acknowledgements

This work was supported by a grant from MR 2D100 Bio/Nano Architectures (UNM). Support for AFRL work was provided by the Air Force Office of Scientific Research and the AFRL-Materials and Manufacturing Directorate.

References

[1] J.M. Abad, M. Gass, A. Bleloch, D.J. Schiffrin, J. Am. Chem. Soc. 131 (2009) 10229.
[2] S. Barton, J. Gallaway, P. Atanassov, Chem. Rev. 104 (2004) 4867.
[3] M. Cooney, V. Svoboda, C. Lau, G. Martin, S. Minteer, Energy Environ. Sci. 1 (2008) 320.
[4] F. Davis, S. Higson, Biosens. Bioelectron. 22 (2007) 1224.
[5] A. Ghindilis, P. Atanasov, E. Wilkins, Electroanalysis 9 (1997) 661.
[6] K. Kano, T. Ikeda, Denki Kagaku Oyobi Kogyo Butsuri Kagaku 71 (2003) 86.
[7] S. Minteer, B. Liaw, M. Cooney, Curr. Opin. Biotechnol. 18 (2007) 228.
[8] A. Sarma, P. Vatsyayan, P. Goswami, S. Minteer, Biosens. Bioelectron. 24 (2009) 2313.
[9] G. Sayler, M. Simpson, C. Cox, Curr. Opin. Microbiol. 7 (2004) 267.
[10] S. Shleev, J. Tkac, A. Christenson, T. Ruzgas, A. Yaropolov, J. Whittaker, L. Gorton, Biosens. Bioelectron. 20 (2005) 2517.
[11] I. Willner, B. Willner, E. Katz, Bioelectrochemistry 70 (2007) 2.
[12] A. Heller, Anal. Bioanal. Chem. 385 (2006) 469.
[13] E. Katz, A. Shipway, I. Willner, Handbook of fuel cells—fundamentals, technology and applications, in: W. Vielstich, H. Gasteiger, A. Lamm (Eds.), Fundamentals and Survey of Systems, vol. 1, John Wlley & Sons, Hoboken, NJ, 2003, p. 355.
[14] C. Vaz-Dominguez, S. Campuzano, O. Ruediger, M. Pita, M. Gorbacheva, S. Shleev, V. Fernandez, A. De Lacey, Biosens. Bioelectron. 24 (2008) 531.
[15] I. Berezin, V. Bogdanovskaya, S. Varfolomeev, M. Tarasevich, A. Yaropolov, Doklady Akademii Nauk SSSR 240 (1978) 615.
[16] A. Benniston, A. Harriman, Coord. Chem. Rev. 252 (2008) 2528.
[17] B. Hassler, R. Worden, Biosens. Bioelectron. 21 (2006) 2146.
[18] D. Ivnitski, B. Branch, P. Atanassov, C. Apblett, Electrochem. Commun. 8 (2006) 1204.
[19] N. Lebedev, S. Trammell, A. Spano, E. Lukashev, I. Griva, J. Schnur, J. Am. Chem. Soc. 128 (2006) 12044.
[20] A. Ramanavicius, A. Ramanaviciene, Fuel Cells 9 (2009) 25.
[21] H. Shin, S. Cho, A. Heller, C. Kang, J. Electrochem. Soc. 156 (2009) F87.
[22] T. Balkenhohl, S. Adelt, R. Dronov, F. Lisdat, Electrochem. Commun. 10 (2008) 914.
[23] C. Blanford, C. Foster, R. Heath, F. Armstrong, Faraday Discuss. 140 (2009) 319.
[24] J. Gallaway, I. Wheeldon, R. Rincon, P. Atanassov, S. Banta, S. Barton, Biosens. Bioelectron. 23 (2008) 1229.
[25] M. Pita, S. Shleev, T. Ruzgas, V. Fernández, A. Yaropolov, L. Gorton, Electrochem. Commun. 8 (2006) 747.
[26] S. Shleev, A. Jarosz-Wilkolazka, A. Khalunina, O. Morozova, A. Yaropolov, T. Ruzgas, L. Gorton, Bioelectrochemistry 67 (2005) 115.

[27] S. Shleev, Y. Wang, M. Gorbacheva, A. Christenson, D. Haltrich, R. Ludwig, T. Ruzgas, L. Gorton, Electroanalysis 20 (2008) 963.
[28] K. Szot, W. Nogala, J. Niedziolka-Jönsson, M. Jönsson-Niedziolka, F. Marken, J. Rogalski, C. Kirchner, G. Wittstock, M. Opallo, Electrochim. Acta 54 (2009) 4620.
[29] M. Tarasevich, V. Bogdanovskaya, A. Kapustin, Electrochem. Commun. 5 (2003) 491.
[30] S. Tsujimura, Y. Kamitaka, K. Kano, Fuel Cells 7 (2007) 463.
[31] S. Tsujimura, K. Kano, T. Ikeda, J. Electroanal. Chem. 576 (2005) 113.
[32] S. Varfolomeev, I. Kurochkin, A. Yaropolov, Biosens. Bioelectron. 11 (1996) 863.
[33] R. Marcus, N. Sutin, Biochim. Biophys. Acta 811 (1985) 265.
[34] E. Solomon, R. Szilagyi, S. George, L. Basumallick, Chem. Rev. 104 (2004) 419.
[35] R. Marcus, Rev. Mod. Phys. 65 (1993) 599.
[36] A. Messerschmidt, H. Luecke, R. Huber, J. Mol. Biol. 230 (1993) 997.
[37] K. Piontek, M. Antorini, T. Choinowski, J. Biol. Chem. 277 (2002) 37663.
[38] E. Solomon, U. Sundaram, T. Machonkin, Chem. Rev. 96 (1996) 2563.
[39] C. Leger, F. Lederer, B. Guigliarelli, P. Bertrand, J. Am. Chem. Soc. 128 (2006) 180.
[40] T. Machonkin, E. Solomon, J. Am. Chem. Soc. 122 (2000) 12547.
[41] L. Rulisek, E. Solomon, U. Ryde, Inorg. Chem. 44 (2005) 5612.
[42] S. Tsujimura, H. Tatsumi, J. Ogawa, S. Shimizu, K. Kano, T. Ikeda, J. Electroanal. Chem. 496 (2001) 69.
[43] S. Shleev, M. Pita, A. Yaropolov, T. Ruzgas, L. Gorton, Electroanalysis 18 (2006) 1901.
[44] B. Reinhammar, T. Vänngård, Eur. J. Biochem. 18 (1971) 463.
[45] A. Christenson, S. Shleev, N. Mano, A. Heller, L. Gorton, Biochim. Biophys. Acta: Bioenerg. 1757 (2006) 1634.
[46] K. Schubert, G. Goebel, F. Lisdat, Electrochim. Acta 54 (2009) 3033.
[47] F. Xu, W. Shin, S. Brown, J. Wahleithner, U. Sundaram, E. Solomon, Biochim. Biophys. Acta Prot. Struct. Mol. Enzymol. 1292 (1996) 303.
[48] K. Murata, N. Nakamura, H. Ohno, Electroanalysis 19 (2007) 530.
[49] T. Sakurai, Chem. Lett. 25 (1996) 481.
[50] R. Santucci, T. Ferri, L. Morpurgo, I. Savini, L. Avigliano, Biochem. J. 332 (1998) 611 (London).
[51] A. Kranich, H. Ly, P. Hildebrandt, D. Murgida, J. Am. Chem. Soc. 130 (2008) 9844.
[52] E. Petrov, V. Teslenko, V. May, Phys. Rev. E 68 (2003) 61916.
[53] F. Armstrong, J. Chem. Soc., Dalton Trans. 2002 (2002) 661.
[54] C. Leger, S. Elliott, K. Hoke, L. Jeuken, A. Jones, F. Armstrong, Biochemistry 42 (2003) 8653.
[55] J. Rusling, R. Forster, J. Colloid Interface Sci. 262 (2003) 1.
[56] K. Lebed, G. Pyka-Fosciak, J. Raczkowska, M. Lekka, J. Styczen, J. Phys.: Condens. Matter 17 (2005) 1447.
[57] T. Fisher, A. Oberhauser, M. Carrion-Vazquez, P. Marszalek, J. Fernandez, Trends Biochem. Sci. 24 (1999) 379.
[58] H. Li, A. Oberhauser, S. Fowler, J. Clarke, J. Fernandez, Proc. Natl. Acad. Sci. 97 (2000) 6527.
[59] D. Müller, C. Schoenenberger, F. Schabert, A. Engel, J. Struct. Biol. 119 (1997) 149.
[60] S. Scheuring, P. Ringler, M. Borgnia, H. Stahlberg, D. Müller, P. Agre, A. Engel, EMBO J. 18 (1999) 4981.
[61] K. Gonzalez Arzola, Y. Gimeno, M.C. Arevalo, M.A. Falcon, A. Hernandez Creus, Bioelectrochemistry 79 (2010) 17.
[62] R.D. Vigil, R.M. Ziff, J. Chem. Phys. 91 (1989) 2599.
[63] S. Shleev, A. Christenson, V. Serezhenkov, D. Burbaev, A. Yaropolov, L. Gorton, T. Ruzgas, Biochem. J. 385 (2005) 745.
[64] D. Ivnitski, P. Atanassov, Electroanalysis 19 (2007) 2307.
[65] O. Farver, I. Pecht, Proc. Natl. Acad. Sci. 89 (1992) 8283.
[66] D. Ivnitski, K. Artyushkova, P. Atanassov, Bioelectrochemistry 74 (2008) 101.
[67] I. Bento, L. Martins, G. Lopes, M. Carrondo, P. Lindley, Dalton Trans. 2005 (2005) 3507.
[68] B. Reinhammar, Multi-copper oxidases, in: A. Messerschmidt (Ed.), World Scientific, 1997, p. 167.
[69] E. Solomon, A. Augustine, J. Yoon, Dalton Trans. 2008 (2008) 3921.
[70] P. Kyritsis, A. Messerschmidt, R. Huber, G. Salmon, A. Sykes, J. Chem. Soc., Dalton Trans. (1993) 731.
[71] S. Lee, S. George, W. Antholine, B. Hedman, K. Hodgson, E. Solomon, J. Am. Chem. Soc. 124 (2002) 6180.
[72] J. Yoon, B.D. Liboiron, R. Sarangi, K.O. Hodgson, B. Hedman, E.I. Solomon, Proc. Natl. Acad. Sci. 104 (2007) 13609.
[73] A. Augustine, M. Kragh, R. Sarangi, S. Fujii, B. Liboiron, C. Stoj, D. Kosman, K. Hodgson, B. Hedman, E. Solomon, Biochemistry 47 (2008) 2036.
[74] L. Davis, B. Drews, H. Yue, D. Waldeck, K. Knorr, R. Clark, J. Phys. Chem. C 112 (2008) 6571.
[75] O. Koroleva, E. Stepanova, V. Gavrilova, V. Biniukov, A. Pronin, Biochemistry 66 (2001) 960 (Moscow).
[76] R. Malkin, B. Malmstrom, T. Vanngard, Eur. J. Biochem. 7 (1969) 253.
[77] A. Messerschmidt, A. Rossi, R. Ladenstein, R. Huber, M. Bolognesi, G. Gatti, A. Marchesini, R. Petruzzelli, A. Finazzi Agro, J. Mol. Biol. 206 (1989) 513.
[78] J. Cole, L. Avigliano, L. Morpurgo, E. Solomon, J. Am. Chem. Soc. 113 (1991) 9080.
[79] J. Cole, P. Clark, E. Solomon, J. Am. Chem. Soc. 112 (1990) 9534.
[80] L. Santagostini, M. Gullotti, L. De Gioia, P. Fantucci, E. Franzini, A. Marchesini, E. Monzani, L. Casella, Int. J. Biochem. Cell Biol. 36 (2004) 881.
[81] T. Sakurai, K. Kataoka, Chem. Rec. 7 (2007) 220.
[82] A. Shimizu, J.-H. Kwon, T. Sasaki, T. Satoh, N. Sakurai, T. Sakurai, S. Yamaguchi, T. Samejima, Biochemistry 38 (1999) 3034.